Title:

Nuclear GAPDH cascade mediates pathological cardiac hypertrophy

Authors:

Manling Zhang[1,*], Taro Kariya[1*], Genri Numata[2*], Hideyuki Sasaki[1,*], Masayuki Sasaki[1], Adriana Ramos[3], Shun Nakamura[2,4], Masaki Iwakiri[5] , Norimichi Koitabashi[1], Guangshuo Zhu[1], Tsuyoshi Tsujimura[3], Dong-ik Lee[1], Carlos Tristan[3], Neelam Shahani[3], Yukihiro Tsuchiya[6], Hanna Jaaro-Peled[3], Tetsuo Sasano[4], Barbara Slusher[7,8], David A. Kass[1], Toshiaki Saitoh[9], Koko Ishizuka[3], Akira Sawa[3,8,10,11#], and Eiki Takimoto[1,2#]

Affiliations:

[1]Division of Cardiology, Departments of [3]Psychiatry, [7]Neurology, [8]Neuroscience, [10]Biomedical Engineering, Johns Hopkins University School of Medicine

[11]Department of Mental Health, Johns Hopkins University Bloomberg School of Public Health

Departments of [2]Cardiovascular Medicine and [5]Anesthesiology,

University of Tokyo School of Medicine

[4]Department of Cardiovascular Medicine, Tokyo Medical and Dental University

[6]Departments of Pharmacology, Showa Pharmaceutical University

[9]Department of Pharmaceutical Sciences, Nihon Pharmaceutical University

[*]These four authors contributed equally to this work

[#]Corresponding authors: etakimo1@jhmi.edu, asawa1@jhmi.edu

One-sentence summary:

Non-glycolytic function of GAPDH critically regulates heart homeostasis and mediates cardiac pathological hypertrophy

Abstract:

Pathological stressors disrupt cellular homeostasis, causing various diseases. We report a non-glycolytic role for glyceraldehyde-3-phosphate dehydrogenase (GAPDH) in the pathological growth response of the heart. In cellular and animal models for cardiac hypertrophy, nuclear translocation of GAPDH was elicited in cardiac myocytes, followed by activation of p300 histone acetyl-transferase (HAT), an inducer of heart hypertrophy gene programs. The hypertrophy was inhibited by a compound antagonizing the nuclear GAPDH cascade. In mice with selective deletion of GAPDH's nuclear function in cardiac myocytes, the stress-induced cardiac hypertrophy and functional deficits were normalized. Nuclear GAPDH cascade plays a pivotal role in stress response/homeostatic control in the heart. GAPDH may act as a key homeostatic mediator in living organisms through its stress-responsive nuclear translation.

Main Text:

Besides glycolytic function, glyceraldehyde-3-phosphate dehydrogenase (GAPDH) has multiple functions, one being the mediation of neural cell death by translocating to the nucleus (*1-5*). The nuclear GAPDH cascade is triggered by a specific oxidation/*S*-nitrosylation of GAPDH at cysteine-150 (C150), which enables the interaction of the pool of GAPDH with Siah1 (*6, 7*). The protein complex translocates to the nucleus where GAPDH affects p300, p53, and p53 upregulated modulator of apoptosis (PUMA), resulting in cell death. In this cascade, only a small fraction of GAPDH is converted to a signaling molecule, and the overall change in cytosolic and glycolytic GAPDH is negligible (*6, 8*). A major knowledge gap is whether this signaling pathway simply leads to cell death by sensing cellular stress at GAPDH-C150, or has more broad and diverse roles in a context-dependent manner.

The heart is among the organs with the highest expression of GAPDH (*9*), which has been simply thought to play a "house keeping" glycolytic role in this organ. The heart develops hypertrophy or abnormal growth in response to pathological stress, which can ultimately result in the organ failure (*10*). Indeed, cardiac hypertrophy and failure is a leading cause of death worldwide, imposing an enormous burden on society (*11*). Although p300 has been implicated in this pathophysiology (*12, 13*), the overall significance and its regulatory mechanism remain elusive. We hypothesize that nuclear GAPDH-p300 cascade may mediate this stress response, which disrupts critical homeostasis of cardiac myocytes and causes hypertrophic growth.

To address this question, we used a mouse model of pressure-overload cardiac hypertrophy induced by transverse aortic constriction (TAC) (*14*). In this model, cardiac hypertrophy is developed at 7 to 10 days after TAC, transitioning to failure in 63 days after TAC. The histone acetyl transferase (HAT) activity of p300 was markedly increased in TAC hearts at

10 days after the constriction (TAC 10D), and remained high at 63 days (TAC 63D) (**Fig. 1A**), which was associated with nuclear accumulation of GAPDH in cardiac myocytes isolated from TAC hearts, as detected by immunostaining (**Fig. 1B**). Nuclear GAPDH accumulation was confirmed by protein subcellular fractionation analysis in the heart tissues (**Fig. 1C**). GAPDH in the nuclear fraction was increased in both TAC 10D and TAC 63D hearts, but not in sham hearts, while GAPDH in the cytosol fraction was unaltered under all conditions (**Fig. 1C**). These results are consistent with our hypothesis that TAC elicits nuclear translocation of GAPDH followed by activation of p300. Bbc3 (the gene encoding PUMA) expression was unchanged in TAC 10D hearts (**fig. S1**), indicating that the mechanism involving nuclear GAPDH in the heart is different from ones previously described (*1-4*).

To test this possibility, we first employed a pharmacological approach to block the nuclear GAPDH cascade. We previously reported that deprenyl, a monoamine oxidase (MAO) inhibitor, and its structural analogue could selectively block the nuclear GAPDH cascade in cells by inhibiting GAPDH-Siah1 protein interaction (*15*). We performed extended screening of structural analogues of deprenyl, and identified more potent and selective blockers of GAPDH-Siah1 binding (*16*). One of the most promising compounds was (1R, 3R)-1, 3-dimethyl-2-propargyl-1, 2, 3, 4-tetrahydroisoquinoline (designated RR in the present manuscript) (**Fig. 2A**). While deprenyl's MAO inhibitory action could elicit adverse cardiovascular effects due to excess levels of catecholamines and serotonin (*17, 18*), RR did not inhibit MAO-A/B at a wide range of concentrations in cardiac myocytes (**Fig. 2B**). Moreover, RR did not affect GAPDH glycolytic activity in cardiac myocytes at 1 nM (**Fig. 2C**), the dose used in our subsequent studies. Comprehensive *in vitro* screening of off-target activities revealed no significant interaction of RR with receptors, transporters and enzymes at the concentration of 1 μM, which is 1,000-fold

higher compared with the concentration at which GAPDH-Siah1 binding was inhibited (**table S1**). These results support the high specificity of RR in inhibiting the GAPDH-Siah1 binding.

We tested the role of nuclear GAPDH cascade in a cardiac cellular hypertrophy model induced by Gq signal stimulation that is a central trigger for pathological hypertrophy response and oxidative stress (*19-23*). Immunofluorescent analysis revealed that stimulation of cardiac myocytes with a Gq agonist endothelin 1 (ET1) (0.05 μM, 48 h) induced nuclear translocation of GAPDH, and that RR blocked the translocation (**Fig. 3, A and B**). Consistent with the ET1-elicited translocation, accumulation of sulfonated GAPDH [reflecting oxidized nuclear GAPDH (*6*)] was observed in the nucleus, which was also blocked by RR (**fig. S2, A and B**). Augmented p300 activity is known to lead to the activation of cardiac hypertrophic gene program through increasing the transcriptional activity of myocyte enhancer factor 2 (MEF2) (*24-26*). ET1 increased the levels of p300 acetylation [reflecting p300 HAT activity (*27*)] and the activity of MEF2 (**Fig. 3C**), and induced robust cellular hypertrophic response including increases in cell surface area, protein synthesis assayed by [^{3}H]leucine uptake, and Nppb [the gene encoding B-type natriuretic peptide (BNP)] expression (**Fig. 3D**). Notably, under this condition, Bbc3 mRNA expression was unchanged (**fig. S2C**). Importantly, all of these changes were attenuated by RR (**Fig. 3, A-D**). These results provide pharmacological evidence that the GAPDH-p300-MEF2 cascade, which is independent of the PUMA-mediated death signaling, plays a crucial role in cardiac hypertrophic response.

To determine the significance of the nuclear GAPDH cascade *in vivo* and explore a novel therapeutic strategy for cardiac hypertrophy, we tested the RR compound in the TAC model (see **Fig. 1**). Daily treatment with RR (0.25 mg/kg/day i.p.) that was initiated at the induction of TAC markedly reduced the levels of nuclear GAPDH and p300 HAT activity in TAC 10D hearts (**Fig.**

3E), and ameliorated cardiac hypertrophy remodeling *in vivo*, as assessed by histology, heart weight, and cardiac myocytes size (**Fig. 3, F and G**) and pathological gene expression profiles (**fig. S3, A and B**). RR treatment also improved TAC-induced cardiac functional impairment (reduction in FS, fractional shortening) and chamber enlargement (increase in LV-EDD, left ventricular end-diastolic dimension), assessed by echocardiography (**Fig. 3H**). An invasive hemodynamic study using pressure volume (PV) loop analyses further revealed improvement of cardiac systolic (dP/dtmax: maximum first derivatives of LV pressure) and diastolic (Tau) performance with RR treatment despite sustained pressure-overload [shown by peak LV pressure (LVP)] and no change in heart rate (**Fig. 3I and fig. S3C**). These results indicate that the RR compound is effective in blocking the nuclear GAPDH cascade and consequent changes in cardiac hypertrophy/remodeling and function *in vivo*.

In most clinical settings, treatment is started only after pathological changes have occurred. Thus, we next tested the efficacy of RR treatment in pre-existing cardiac hypertrophy. Hearts exposed to pressure-overload for 7 days (TAC 7D) developed hypertrophy with 50% increase in left ventricular (LV) mass, compared with sham controls, by echocardiography. Two weeks of RR treatment to TAC 7D hearts significantly inhibited further increase in LV mass when compared with vehicle treatment (**Fig. 3J**). At the cellular and molecular levels, this treatment resulted in smaller cardiac myocytes (**Fig. 3J and fig. S3D**) and improved Nppb expression profile (**fig. S3D**).

We further validated this mechanism employing molecular intervention. The mouse lysine residue K225 (corresponding to human K227) of GAPDH is crucial for its binding to Siah1: the replacement of K225 with alanine in GAPDH (K225A mutant) interferes with the nuclear GAPDH cascade, but maintains its glycolytic activity (*6*). Accordingly, we generated a

cardiac myocyte-specific knock-in mouse harboring the GAPDH K225A mutation (**Fig. 4A, fig. S, 4A and B**), using the tamoxifen-inducible Cre-loxP system, and examined the hypertrophic response of the heart to pressure overload (TAC). In GAPDH-K225A hearts, the mutated protein was expressed in cardiac myocytes (**fig. S4C**), but GAPDH-Siah1 binding was virtually abrogated during pressure-overload (**Fig. 4B**). GAPDH-K225A hearts revealed a markedly alleviated hypertrophic response to TAC as determined by histology, heart weight, and cardiac myocytes size (**Fig. 4C, and D**), with no translocation of GAPDH-K225A into the nucleus (**fig. S4D**). Importantly, this blunted cardiac hypertrophic response was associated with preserved LV cardiac function and chamber size, as assessed by echocardiographic fractional shortening (%FS) and LV-EDD (**Fig. 4E**). Consistently, comprehensive PV loop analyses revealed that cardiac systolic (dP/dtmax/IP: maximum first derivatives of LV pressure normalized to instantaneous pressure) and diastolic (Tau) performance was preserved in GAPDH-K225A TAC hearts, while both were impaired in wild-type (WT) TAC hearts (**Fig. 4F**). In contrast, cardiac afterload (peak LVP) was similarly elevated in both GAPDH-K225A and WT hearts (**fig S5**). At the molecular level, we did not observe the TAC-induced, heart hypertrophy-associated pathology (assayed by Nppb and Myh7/6 expressions) or abnormal calcium handling regulation (assayed by Atp2a2 and Pln expression) in GAPDH-K225A TAC hearts. Notably, apoptotic signal induction (assayed by Bbc3 and Bnip3l expressions) was not evident in both GAPDH-K225A and WT hearts in response to TAC (**fig S6**). These results indicate that GAPDH-K225A hearts better adapted to the pathological stressor and pressure-overload, compared to WT. Altogether, the inhibition of the nuclear GAPDH cascade, either by pharmacological or molecular intervention, consistently ameliorated pathological hypertrophic remodeling.

In the present study, we demonstrate a pivotal role for the nuclear GAPDH cascade pathway in cardiac hypertrophy in response to pathological stressors in which GAPDH non-enzymatically senses stress and induces hypertrophic gene programing. Thus, we propose the nuclear GAPDH cascade as an essential stress mediator in the heart that could be targeted to maintain cardiac homeostasis. Interestingly, the molecular mechanism elicited by the nuclear translocation of GAPDH in the heart is distinct from the cascades reported in neurons in the brain, implying the general and tissue/context-specific roles of the nuclear GAPDH cascade in stress response. It would be intriguing to identify the roles for this cascade in other organs and under diverse stress situations.

GAPDH may be a key homeostatic mediator in living organisms, given its robust expression in many tissues/organs. We note that recent reports have also underscored GAPDH as a stress sensor but in a different mechanism from its nuclear translation. For example, GAPDH has been reported to sense reduced glycolytic flux, bind to the AU-rich region in the 3' UTR of cytokine mRNA, and suppress its translation in T cells, indicating that GAPDH works as an important molecular sensor that coordinates glycolytic metabolism with effector T cell function (*28*). GAPDH is also involved in an inflammatory/immune process when dimethyl fumarate (DMF) succinates GAPDH and down-regulates its glycolytic activity, which would be a mechanism for DMF's treatment action to autoimmune diseases (*29*).

In the present study, we provide a novel compound that specifically and potently blocks the nuclear GAPDH cascade, which opens a window for a potential therapeutic avenue. Given that heart hypertrophy is still limited in its treatment, we hope that the compound will lead to a novel drug discovery for this difficult heart condition. Since this cascade is likely to be involved

in a variety of pathological conditions in which organ homeostasis is disturbed, it may have broad clinical applicability.

References:

1. D. M. Chuang, C. Hough, V. V. Senatorov, Glyceraldehyde-3-phosphate dehydrogenase, apoptosis, and neurodegenerative diseases. *Annu Rev Pharmacol Toxicol* **45**, 269-290 (2005).
2. M. A. Sirover, On the functional diversity of glyceraldehyde-3-phosphate dehydrogenase: biochemical mechanisms and regulatory control. *Biochim Biophys Acta* **1810**, 741-751 (2011).
3. D. Zala *et al.*, Vesicular glycolysis provides on-board energy for fast axonal transport. *Cell* **152**, 479-491 (2013).
4. N. Shahani, A. Sawa, Nitric oxide signaling and nitrosative stress in neurons: role for S-nitrosylation. *Antioxid Redox Signal* **14**, 1493-1504 (2011).
5. C. Tristan, N. Shahani, T. W. Sedlak, A. Sawa, The diverse functions of GAPDH: views from different subcellular compartments. *Cellular signalling* **23**, 317-323 (2011).
6. M. R. Hara *et al.*, S-nitrosylated GAPDH initiates apoptotic cell death by nuclear translocation following Siah1 binding. *Nat Cell Biol* **7**, 665-674 (2005).
7. M. R. Hara, M. B. Cascio, A. Sawa, GAPDH as a sensor of NO stress. *Biochim Biophys Acta* **1762**, 502-509 (2006).
8. N. Sen *et al.*, Nitric oxide-induced nuclear GAPDH activates p300/CBP and mediates apoptosis. *Nat Cell Biol* **10**, 866-873 (2008).
9. T. Brattelid *et al.*, Reference gene alternatives to Gapdh in rodent and human heart failure gene expression studies. *BMC Mol Biol* **11**, 22 (2010).
10. J. A. Hill, E. N. Olson, Cardiac plasticity. *The New England journal of medicine* **358**, 1370-1380 (2008).

11. S. Neubauer, The failing heart--an engine out of fuel. *The New England journal of medicine* **356**, 1140-1151 (2007).

12. R. J. Gusterson, E. Jazrawi, I. M. Adcock, D. S. Latchman, The transcriptional co-activators CREB-binding protein (CBP) and p300 play a critical role in cardiac hypertrophy that is dependent on their histone acetyltransferase activity. *J Biol Chem* **278**, 6838-6847 (2003).

13. T. Yanazume, T. Morimoto, H. Wada, T. Kawamura, K. Hasegawa, Biological role of p300 in cardiac myocytes. *Mol Cell Biochem* **248**, 115-119 (2003).

14. E. Takimoto *et al.*, Chronic inhibition of cyclic GMP phosphodiesterase 5A prevents and reverses cardiac hypertrophy. *Nat.Med.* **11**, 214-222 (2005).

15. M. R. Hara *et al.*, Neuroprotection by pharmacologic blockade of the GAPDH death cascade. *Proc Natl Acad Sci U S A* **103**, 3887-3889 (2006).

16. T. Saitoh, K. Shikiya, Y. Horiguchi, T. Sano, Super acid-induced Pummerer-type cyclization reaction: improvement in the synthesis of chiral 1,3-dimethyl-1,2,3,4-tetrahydroisoquinolines. *Chem Pharm Bull (Tokyo)* **51**, 667-672 (2003).

17. M. Wimbiscus, O. Kostenko, D. Malone, MAO inhibitors: risks, benefits, and lore. *Cleveland Clinic journal of medicine* **77**, 859-882 (2010).

18. M. R. Bristow, Treatment of chronic heart failure with beta-adrenergic receptor antagonists: a convergence of receptor pharmacology and clinical cardiology. *Circulation research* **109**, 1176-1194 (2011).

19. E. Takimoto, D. A. Kass, Role of oxidative stress in cardiac hypertrophy and remodeling. *Hypertension* **49**, 241-248 (2007).

20. T. Ago *et al.*, A redox-dependent pathway for regulating class II HDACs and cardiac hypertrophy. *Cell* **133**, 978-993 (2008).

21. E. Takimoto *et al.*, Regulator of G protein signaling 2 mediates cardiac compensation to pressure overload and antihypertrophic effects of PDE5 inhibition in mice. *J Clin Invest* **119**, 408-420 (2009).

22. N. Wettschureck *et al.*, Absence of pressure overload induced myocardial hypertrophy after conditional inactivation of Galphaq/Galpha11 in cardiomyocytes. *Nat Med* **7**, 1236-1240 (2001).

23. G. W. Dorn, 2nd, T. Force, Protein kinase cascades in the regulation of cardiac hypertrophy. *J Clin Invest* **115**, 527-537 (2005).

24. Y. Kim *et al.*, The MEF2D transcription factor mediates stress-dependent cardiac remodeling in mice. *J Clin Invest* **118**, 124-132 (2008).

25. T. I. Slepak *et al.*, Control of cardiac-specific transcription by p300 through myocyte enhancer factor-2D. *J Biol Chem* **276**, 7575-7585 (2001).

26. J. Q. Wei *et al.*, Quantitative control of adaptive cardiac hypertrophy by acetyltransferase p300. *Circulation* **118**, 934-946 (2008).

27. P. R. Thompson *et al.*, Regulation of the p300 HAT domain via a novel activation loop. *Nat Struct Mol Biol* **11**, 308-315 (2004).

28. C. H. Chang *et al.*, Posttranscriptional control of T cell effector function by aerobic glycolysis. *Cell* **153**, 1239-1251 (2013).

29. M. D. Kornberg *et al.*, Dimethyl fumarate targets GAPDH and aerobic glycolysis to modulate immunity. *Science* **360**, 449-453 (2018).

30. R. Deloux *et al.*, Voluntary Exercise Improves Cardiac Function and Prevents Cardiac Remodeling in a Mouse Model of Dilated Cardiomyopathy. *Frontiers in physiology* **8**, 899 (2017).

31. M. Zhang *et al.*, Myocardial remodeling is controlled by myocyte-targeted gene regulation of phosphodiesterase type 5. *Journal of the American College of Cardiology* **56**, 2021-2030 (2010).

Acknowledgments: We thank Dr. Pamela Talalay and Ms. Lauren Guttman for critical reading of the manuscript. We also thank Ms. Yukiko Lema for organizing the figures and manuscript.

Funding: This work was supported by USPHS grants of HL-093432 (E.T.), MH-084018 (A.S.), MH-094268 Silvio O. Conte center (A.S.), MH-069853 (A.S.), MH-085226 (A.S.), MH-088753 (A.S.), MH-092443 (A.S.), MH-105660 (A.S.), MH-107730 (A.S.), HL-077180 (D.A.K.), HL-059408 (D.A.K.), HL-07227 (M.Z.), F31NS070459 (C.T.), and AHA grant GIA 7700071 (E.T.), Miyata Cardiac Research Promotion Foundation grant (E.T.), AHA post-doctoral fellowship (M.Z.), Stanley (A.S.), RUSK (A.S.), S-R foundations (A.S.), NARSAD (A.S., H.J-P., and N.S.) and Maryland Stem Cell Research Fund (A.S.). Maryland Stem Cell Research Fund (A.S.)

Author contributions: E.T. and A.S. conceptualized all the project. M.Z., T.K., G.N., H.S., M.S., A.R., S.N., M.I., N.K., G.Z., T.T., D.L., C.T., N.S., Y.T., H.J.-P., T.S. and K.I. performed all experiments and analyses. E.T. and A.S. wrote the manuscript. B.S., T.S., and D.A.K. provided critical edits and feedback to the manuscript.

Competing interests: Authors declare that they have no competing interests.

Data and materials availability: All data are available in the main text or the supplementary materials.

Figure 1 | Augmented p300 HAT activity and nuclear accumulation of GAPDH in hypertrophied hearts exposed to chronic pressure-overload (TAC).

A. P300-HAT activity in TAC hearts (n=4 in each group).

B. Representative pictures showing gross anatomy of TAC hearts (upper panels) and immunofluorescent staining for GAPDH in cardiac myocytes isolated from TAC hearts (middle and lower panels). Scale bars, 5 mm (upper panel) and 10 μm (lower panel).

C. Western blots (upper panels) and quantification (bar graphs, n=6 in each group) with fractionated proteins from TAC hearts. TAC 10D, outcome of TAC for 10 days; and TAC 63D, outcome of TAC for 63 days.

*$p<0.05$.

Fig. 2 | A novel compound that blocks GAPDH-Siah1 binding and the nuclear GAPDH cascade.

A. Chemical structure of "(1R, 3R)-1, 3-dimethyl-2-propargyl-1, 2, 3, 4-tetrahydroisoquinoline (RR compound)" in comparison to deprenyl**.**

B. *In vitro* MAO activity assay of RR compound and Deprenyl. Note that RR has no effect on MAO activity in contrast to Deprenyl.

C. Glycolytic activity in cultured rat neonatal cardiac cells exposed to 1 nM RR for 48 h.

Figure 3 | Nuclear translocation of GAPDH in cardiac hypertrophy and its pharmacologic blockade.

A. Immuno-fluorescent staining for GAPDH nuclear translocation in cultured cardiac myocytes exposed to ET1 in the presence or absence of RR compound. Scale bar, 50 μm.

B. Quantification of GAPDH staining. Ratios of average intensity in the nucleus to that in cytosol for GAPDH are shown: 30 cells were analyzed in each group.

C. p300 acetylation and MEF2 activity.

D. Assessment of cardiac myocyte hypertrophy by cell surface area (left), protein synthesis (middle), and Nppb (the gene encoding BNP) expression (right).

E. Nuclear GAPDH amount (left) and p300 HAT activity in TAC hearts with vehicle (Veh) or RR (RR) treatment (right). n=3-4 in each group.

F. Representative cross-sections of hearts (upper panels) and histology (lower panels for WGA staining). Scale bars, 5 mm (upper panel) and 10 μm (lower panel).

G. Assessment of cardiac hypertrophy: heart weight normalized by tibia length (left) and average size of cardiac myocytes assayed by cross-sectional area analysis (right). n=5-7 in each group.

H. Echocardiogram: representative M-mode image (left), fractional shortening (FS) (middle), and left ventricular chamber size at end-diastole (LV-EDD) (right). n=5-7 in each group.

I. Comprehensive cardiac functional assessment from invasive pressure-volume loop analysis: representative loops during preload reduction (left), contractile parameter (dP/dtmax: maximum first derivatives of LV pressure) (middle), and relaxation parameter (Tau) (right). n=5-7 in each group.

J. RR treatment in pre-existing cardiac hypertrophy. Left ventricular mass calculated from echo-cardiogram before [pre-treatment at 7 days after the aortic constriction started (TAC 7D)] and after [post-treatment at 3 weeks after the constriction started (TAC 21D)] treatment (left). Left ventricular mass increase over 2 weeks (ΔLV mass increase) with vehicle or RR treatment (middle), and terminal cardiac myocyte size assayed by cross-sectional area analysis (right). n=5-7 in each group.

*p<0.05.

Figure 4 | The role of nuclear GAPDH cascade in cardiac hypertrophy remodeling, validated by cardiac myocyte-specific selective inactivation of nuclear GAPDH cascade *in vivo*.

A. Design of the GAPDH K225A conditional knock-in model.

B. Heart tissue homogenates (after exposure to 10-day TAC from WT or GAPDH K225A mutant) immunoprecipitated with Siah1 antibody and probed for GAPDH (left panel) and the quantification results (right panel, results from 3 experiments).

C. Representative cross-sections of hearts (upper panels) and histology (lower panels for WGA staining). Scale bars, 5 mm (upper panel) and 10 μm (lower panel).

D. Assessment of cardiac hypertrophy: heart weight normalized to tibia length (left) and average size of cardiac myocytes assayed by cross-sectional area analysis (right). n=5-7 in each group.

E. Echocardiogram: representative M-mode image (left), fractional shortening (FS) (middle) and left ventricular chamber size at end-diastole (LV-EDD) (right). n=5-7 in each group.

F. Comprehensive cardiac functional assessment from invasive pressure-volume loop analysis: representative loops during preload reduction (left), contractile parameter (dP/dtmax/IP: maximum first derivatives of LV pressure normalized to instantaneous pressure) (middle), and relaxation parameter (Tau) (right). n=5-7 in each group.

*p<0.05; **p<0.01.

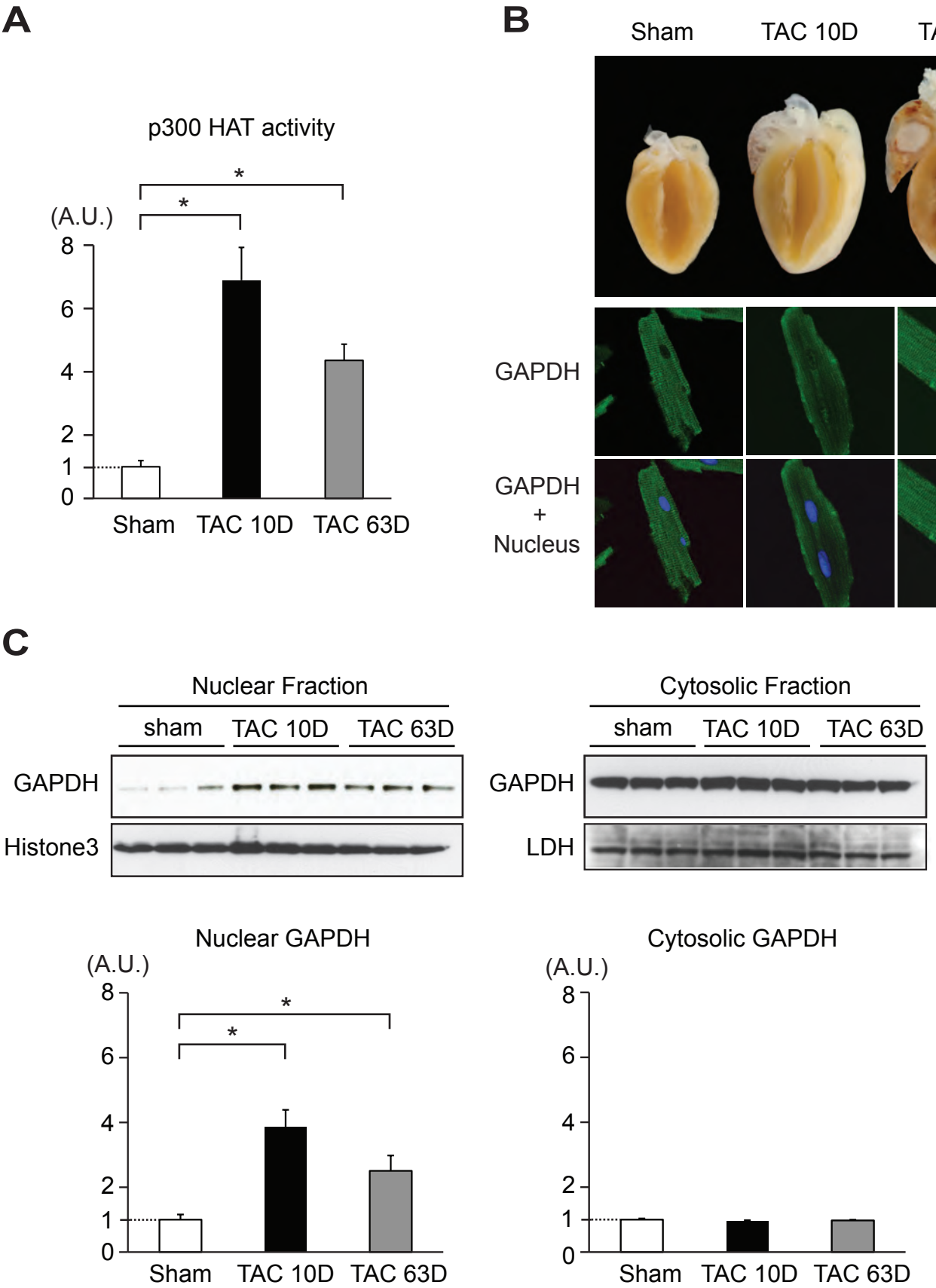
A
p300 HAT activity
(A.U.)
8
6
4
2
1
0
*
*
Sham
TAC 10D
TAC 63D
B
Sham
TAC 10D
TAC 63D
GAPDH
GAPDH
+
Nucleus
C
Nuclear Fraction
sham
TAC 10D
TAC 63D
GAPDH
Histone3
Cytosolic Fraction
sham
TAC 10D
TAC 63D
GAPDH
LDH
Nuclear GAPDH
(A.U.)
8
6
4
2
1
0
*
*
Sham
TAC 10D
TAC 63D
Cytosolic GAPDH
(A.U.)
8
6
4
2
1
0
Sham
TAC 10D
TAC 63D

Fig. 1

A

(1R, 3R)-1, 3-dimethyl-2-propargyl
-1, 2, 3, 4-tetrahydroisoquinoline
(RR compound)

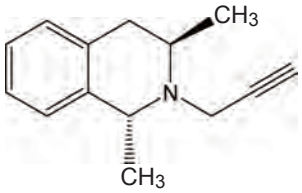

Deprenyl (Dpr)

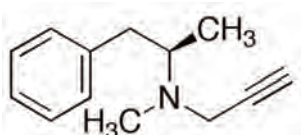

B

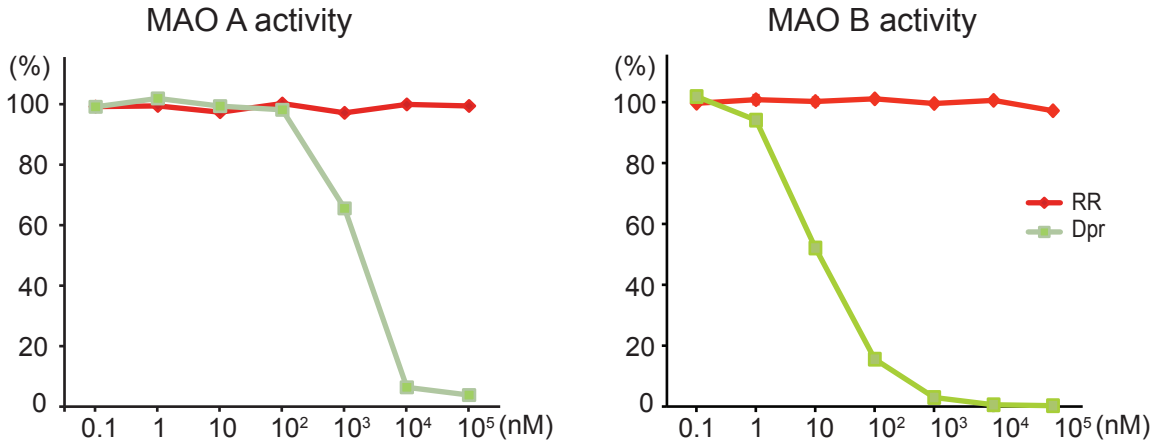

C

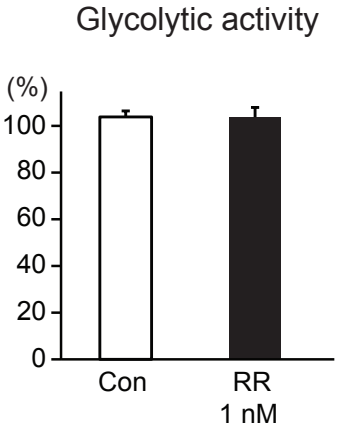

Fig. 2

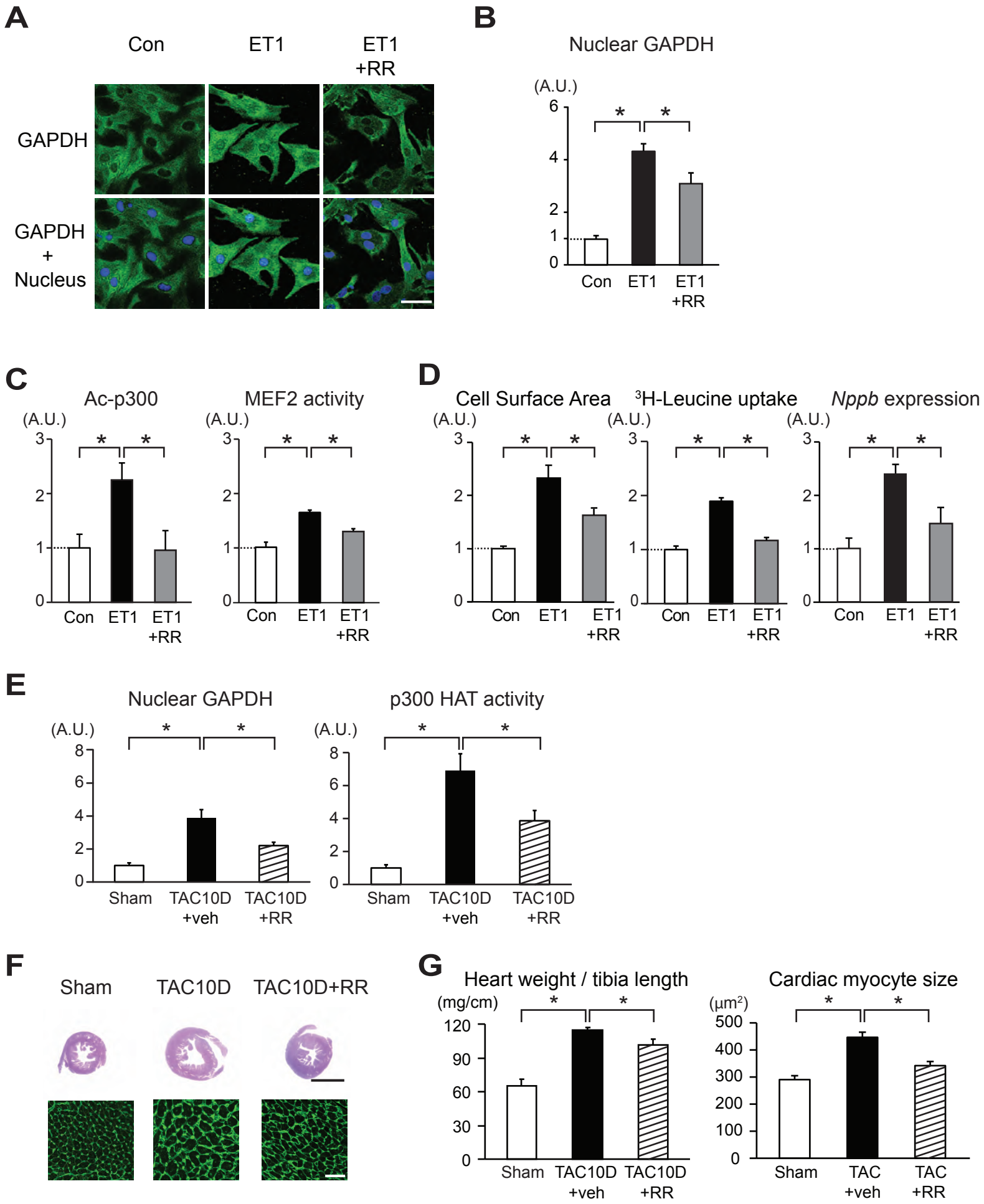
A
Con
ET1
ET1 +RR
GAPDH
GAPDH + Nucleus
B
Nuclear GAPDH
(A.U.)
6
4
2
1
0
*
*
Con
ET1
ET1 +RR
C
Ac-p300
MEF2 activity
(A.U.)
3
2
1
0
*
*
Con
ET1
ET1 +RR
D
Cell Surface Area
3H-Leucine uptake
Nppb expression
(A.U.)
3
2
1
0
*
*
Con
ET1
ET1 +RR
E
Nuclear GAPDH
p300 HAT activity
(A.U.)
8
6
4
2
0
*
*
Sham
TAC10D +veh
TAC10D +RR
F
Sham
TAC10D
TAC10D+RR
G
Heart weight / tibia length
(mg/cm)
120
90
60
30
0
Sham
TAC10D +veh
TAC10D +RR
Cardiac myocyte size
(μm2)
500
400
300
200
100
0
Sham
TAC +veh
TAC +RR

Fig. 3

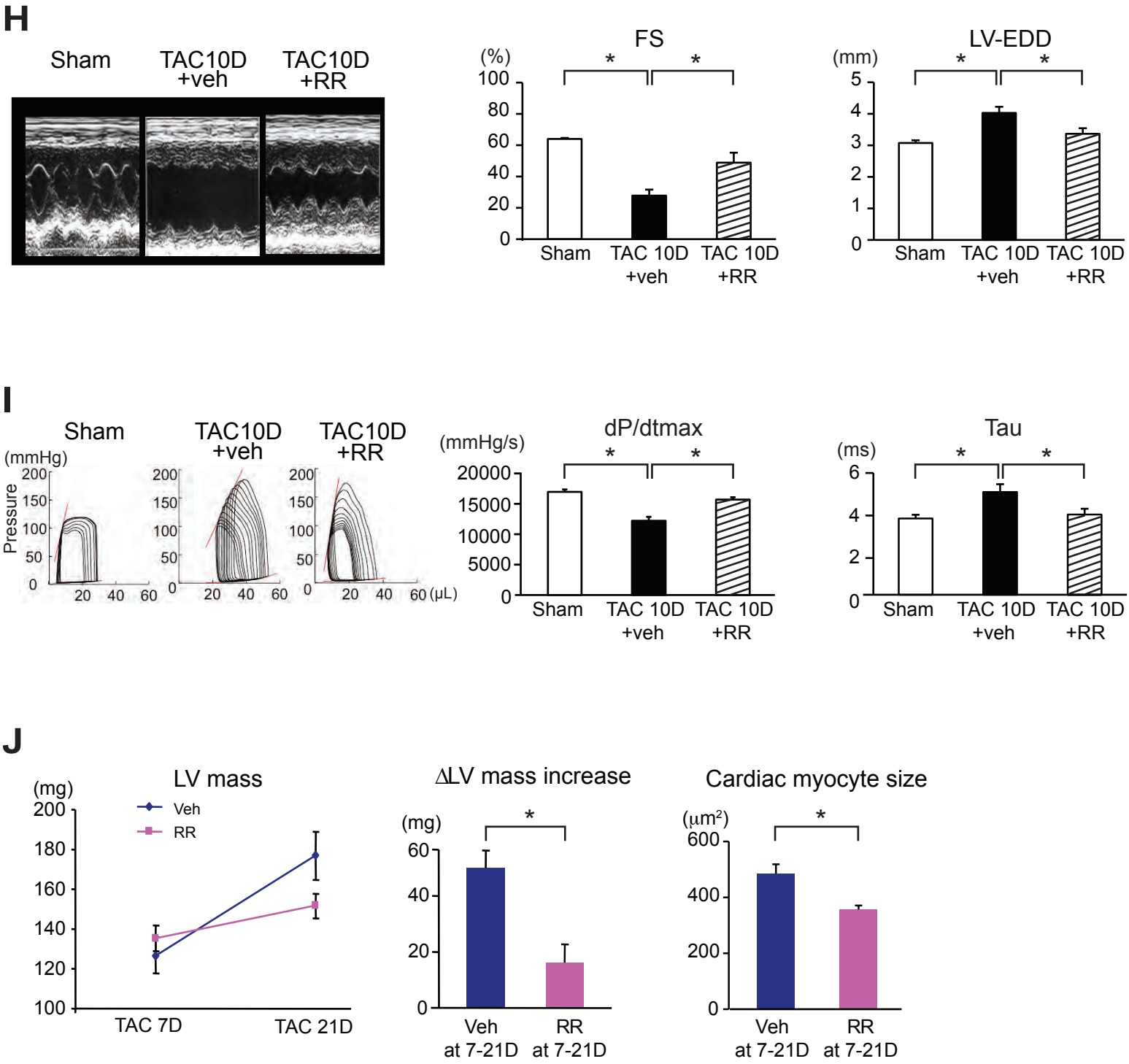
H
Sham
TAC10D +veh
TAC10D +RR
FS
(%)
100
80
60
40
20
0
Sham
TAC 10D +veh
TAC 10D +RR
LV-EDD
(mm)
5
4
3
2
1
0
I
Sham
TAC10D +veh
TAC10D +RR
(mmHg)
Pressure
200
150
100
50
0
20
40
60
(μL)
dP/dtmax
(mmHg/s)
20000
15000
10000
5000
Tau
(ms)
6
J
LV mass
(mg)
Veh
RR
200
180
160
140
120
100
TAC 7D
TAC 21D
ΔLV mass increase
Veh at 7-21D
RR at 7-21D
Cardiac myocyte size
(μm²)
600
400

Fig. 3

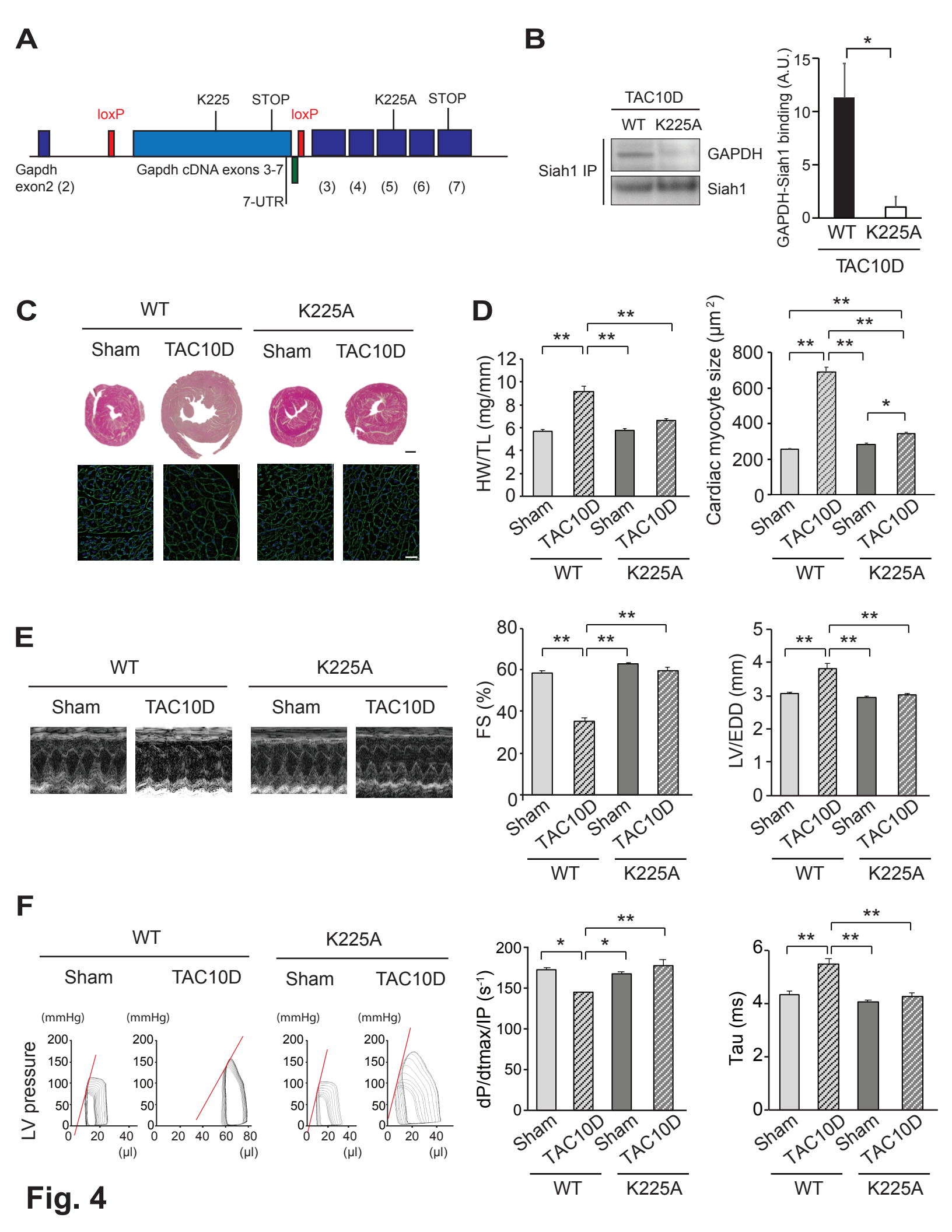
A
loxP
K225
STOP
loxP
K225A
STOP
Gapdh exon2 (2)
Gapdh cDNA exons 3-7
7-UTR
(3) (4) (5) (6) (7)
B
TAC10D
WT K225A
Siah1 IP
GAPDH
Siah1
GAPDH-Siah1 binding (A.U.)
WT K225A
TAC10D
C
WT
K225A
Sham TAC10D Sham TAC10D
D
HW/TL (mg/mm)
Cardiac myocyte size (μm 2)
Sham TAC10D Sham TAC10D
WT K225A
E
WT
K225A
Sham TAC10D Sham TAC10D
FS (%)
LV/EDD (mm)
Sham TAC10D Sham TAC10D
WT K225A
F
WT
K225A
Sham TAC10D Sham TAC10D
(mmHg)
LV pressure
(μl)
dP/dtmax/IP (s-1)
Tau (ms)
Sham TAC10D Sham TAC10D
WT K225A

Fig. 4